

Rapid Prototyping Assisted Design and Development of Inter-Vertebral Implants

J. Chiang, M. Lehmicke, D. Dcosta, X. Hu, F. Lin, W. Sun⁽¹⁾

Department of Mechanical Engineering and Mechanics
Drexel University, Philadelphia, PA 19104

Abstract

This paper presents a case study of applying rapid prototyping in assisting in the design and development of inter-vertebral implants for spine fusions. The major process of design and implant development, its biological and mechanical requirements, the approach for developing a 3D reconstructive vertebral anatomy model, the inter-vertebral implant CAD model, and the integration with a finite element analysis for the implant's structural analysis are presented. The process of 3D Printing of the vertebral anatomy and the inter-vertebral implant is described. The application of the prototyping model in assisting in the inter-vertebral anatomic fitting, in guiding the implant's geometric design, in helping with the virtual surgical planning, and in understanding the implant's mechanical properties and structural stability are discussed.

1. Introduction

Over 1 million operations annually involve bone repair and over 200,000 spine fusion procedures are carried out each year in order to cure various back ailments [1, 2]. Pseudoarthrosis occurs in 10 - 40% of single level fusions, and at a significantly higher rate for multiple level fusions [3]. Current standards of care for spinal fusion involve various implants or grafting techniques. However, these techniques or implants are often limited by their biological or mechanical constraints. For example, autograft, the best grafting process, which takes bone from the patient's own body, is limited by its availability and variation in quality (bone from an osteoporotic patient is not strong graft material), and perhaps most significantly, by its host site morbidity. Allograft, processed from cadavers when or where autograft is not available or practical, has a lower success rate compared to autograft in most settings. In addition, it carries the risk of disease transmission. Due to these limitations, implants have been developed specifically for spinal fusions. The most commonly used implants are normally made from titanium, a biocompatible material that has good mechanical properties. The geometries of inter-vertebral implants also vary, from circular threaded implants (placed with the axis perpendicular to the axis of the spine), to mesh implants (placed with the axis parallel to the axis of the spine), and to implants that are rectangular or "dog boned" in shape. Biomechanical studies have demonstrated that rectangular inter-vertebral implants offer increased stiffness in compression as compared to cylindrical ones [4]. Some surgeons believe that the increased contact area offered by a rectangular inter-vertebral implant may also increase the likelihood of fusion.

From a mechanical point of view, any implant for spinal fusion must provide immediate stability under compression. The implant must remain motionless while transmitting

⁽¹⁾ Corresponding author

compressive forces in order for bone healing to occur. Bone will not grow where there are tensional or bending motions, nor will it grow in the absence of stress. Mechanical stability, however, is not the only factor, certain biological factors must also be present. These factors include the osteogenic cells (that remodel bone), osteoinductive factors (that encourage bone growth), and osteoconductive factors (that provide a frame or scaffold for bone growth). Unfortunately, pure titanium made inter-vertebral implants fail to provide any of these biological factors. On the other hand, although hydroxyapatite has been widely used for coating many orthopedic implants due to its osteoinductive behavior [5-7], it is brittle and fractures easily over time, and therefore, hydroxyapatite is difficult to use alone as an ideal implant material. Furthermore, plasma sprayed hydroxyapatite on the surface of metallic implants may change its compositional properties; the coated hydroxyapatite also produces a modulus mismatch, and frequently the hydroxyapatite coating on the newly formed bone will peel off from the metallic implants and the uniformity of the physical and chemical properties as well as the bioactivity could eventually be lost [8-12].

Recently, a Titanium-Hydroxyapatite (TiHA) composite has been considered as a potential biomaterial that can offer a blended biocompatibility, osteoinductive properties, and mechanical properties for implant application. This paper will report a case study of using rapid prototyping technology, along with enabling computer-aided design and computer-aided engineering (CAD/CAE), medical imaging processing and 3D reconstruction to assist in the design and development of TiHA inter-vertebral implants. The presentation of the paper is organized as follows. Section 2 describes the process of the 3D reconstruction in building vertebral anatomy from computed topography images. The CAD modeling and integrated CAD and CAE simulation in the design development and in the structural analysis of the inter-vertebral implant is presented in Section 3, including the studies on the anatomic fitting of the models and the implant's structural stability in spinal fusions. The major procedures of the 3D Printing and post sintering process for prototyping the vertebral physical model and the implant are described in Section 4. A summary and conclusion are given in Section 5.

2. Three-Dimensional Reconstruction

When considering a reconstructive surgery or implantation, it is often difficult to ascertain the exact nature of the affected internal anatomy. Advances in Computed Tomography (CT) and Magnetic Resonance Imaging (MRI) have led to the generation of 3-Dimensional (3D) representations, or views, for internal anatomies through 3D reconstructive techniques. A general process for 3D reconstruction of an anatomic model from CT or MRI data is described in Figure 1. As shown in the process, the CT or MRI data are extracted through 2D segmentation and 3D region growth to form volumetric image which provides more meaningful and derivative 3D anatomic representation. A 3D anatomic representation produces novel views of patient anatomy while retaining the image voxel intensities that can be used for volume rendering and volumetric representation of 3D anatomic structure. The 3D volumetric representation of anatomic structures can be used to generate a contour based, surface based, or volume based computer modeling through CAD techniques, or to be used to directly produce physical prototype. These CAD and prototyping modeling are very helpful when applied to assist in surgical planning, practice, and education [13].

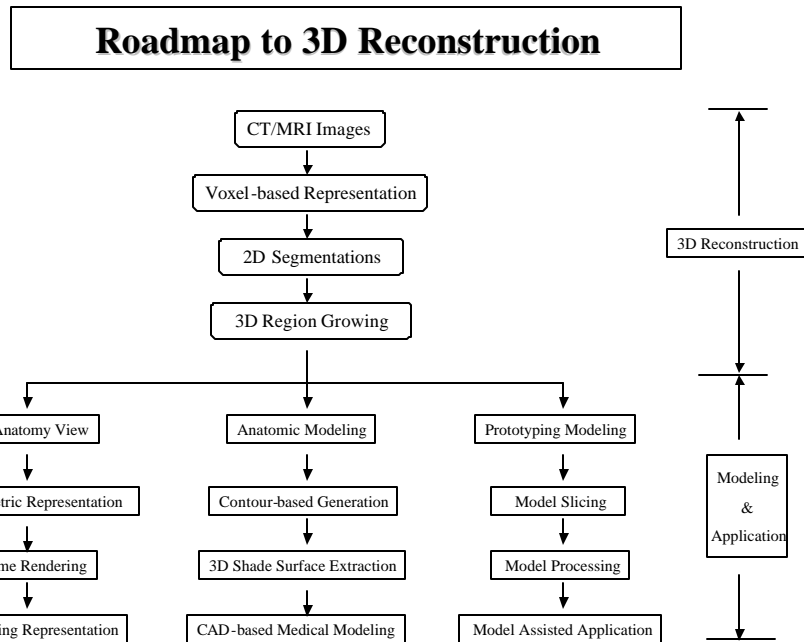


Figure 1: From CT/MRI to 3D reconstruction [13]

In this case study, a CT scan of the spine of an adult human cadaver was used. CT gives excellent resolution of the vertebral bony structures with which the accurate 3D vertebral models can be developed. The geometric and positional accuracy of the vertebral bony structures is critical since the implant will rest between two successive vertebrae and act as an extension of the vertebral bodies. CT data was input into MIMICS, a software package (Materialise Corp., Belgium) used to interface the scanned images and the 3D reconstructive model for vertebral anatomy. MIMICS allows users not only to visualize CT segments but also to edit them as needed, in our case, to create a needed cavity by removing the inter-vertebral disc and to simulate the insertion and placement a suitable implant.

The patient's CT images were imported into *MIMICS*. Factors such as image size, slice thickness, pixel size, and number of images per file were properly defined and the images were organized in order to select the region of interest: two adjacent vertebrae. Directions (anterior, posterior, top, bottom, left, right) were set according to the anatomy. A profile line was drawn transversely across the vertebral body. Based on this profile, a lower threshold value between the value of the cortical wall of the vertebrae and the inside of the vertebral body was set. After setting the threshold, region growing was used to define a yellow mask including the cortical bone regions. A 3D reconstruction of this mask was generated and is shown in Figure 2. Poly-lines were then created and the image was cleaned up to more accurately represent the region of interest. The tubular structure anterior to the vertebral bodies was removed. This structure was probably the aorta or vena cava based on its location. The "filaments" between the vertebral bodies were also removed as these were probably representative osteophytes or the degenerated disc, and in any case, this area would be removed during the surgical procedure. Finally, a clean 3D reconstructive vertebrae representation after removing the soft tissue and the inter-vertebral disc was created as shown in Figure 3. The 3D reconstructive model is further translated into an

stl format to produce rapid prototyping modeling, which will be used to guide the spinal inter-vertebral implant design.

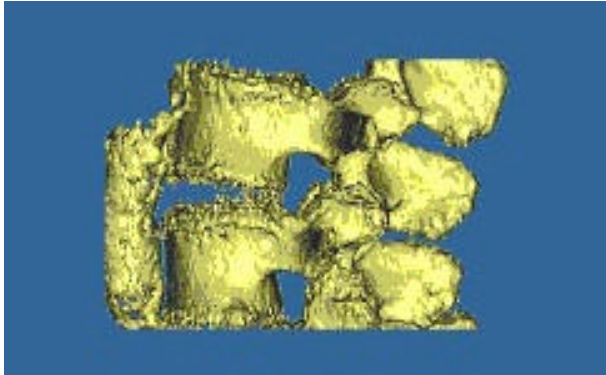


Figure 2: 3D reconstructive vertebrae with soft tissue and inter-vertebrae disc

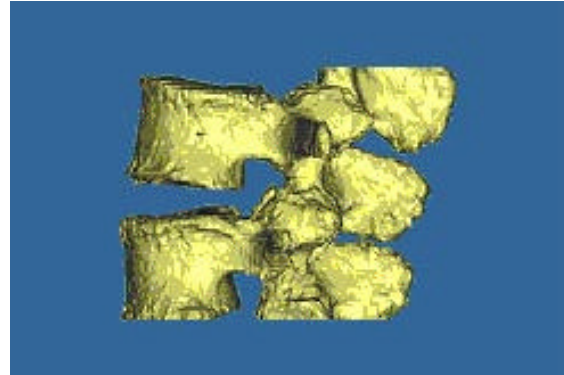


Figure 3: Edited 3D reconstructive vertebrae After removing soft tissue and inter-vertebrae disc

3. Inter-Vertebral Implant Design Modeling and Structural Simulation

The following design considerations were applied in the design and development of the spinal inter-vertebral implant:

1. The inter-vertebral implant must be implantable by using the existing instruments;
2. The size of the implant must anatomically fit within the patient's vertebrae;
3. The implant must be able to withstand the pressures exerted on it by the spine;
4. If needed, allograft or autograft material may be placed inside the implant.

The anatomic compatibility, or the anatomic fit, of the spinal inter-vertebral implant was accomplished by designing the geometry and size of the implant to fit the interior cavity of the vertebrae. The determination of the interior cavity of the vertebrae was achieved by using the 3D reconstructive model developed from the patient's CT imaging. According to the anatomic dimensions, the spinal inter-vertebral implant was designed and the CAD model was generated through Pro/Engineer (Pro/E) 2000i software [Parametric Technology Corporation, Waltham, Massachusetts, 2001]. Using the Pro/E feature and parameteric-based design capability, we defined the implant critical dimensions, such as the height and the contour size of the surfaces, as the parameters which are determined from the patient 3D reconstructive model generated from the CT image, and also on purposely designed the top and bottom surfaces of the inter-vertebral implant with an inclined angle in order to best fit the interior cavity of the customized vertebrae. Representations of the designed implant CAD model and its anatomic fitting are presented in Figure 4 and Figure 5, respectively.

As discussed earlier, titanium is a well-known biomaterial with good mechanical properties, but it is not bioactive, whereas hydroxyapatite is bioactive (osteoconductive), but it is brittle. The combination of hydroxyapatite and titanium, TiHA, may lead to a composite material with desirable biological and mechanical properties. As in any composite material, the properties of TiHA depend on the composition of the constituents. When TiHA is used to make the spinal

inter-vertebral implant, it is important to know its strength and stiffness associated with the given compositions in order to determine whether the designed implant can undertake the applied load after being placed. The analyses to determine the mechanical behavior of the inter-vertebral implant were conducted by using Pro/MECHANICA (Pro/M) [Parametric Technology Corporation, Waltham, Massachusetts, 2001], a finite element analysis software.

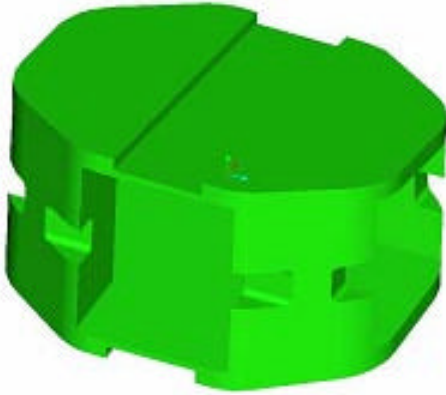


Figure 4: CAD model of the designed inter-vertebral implant

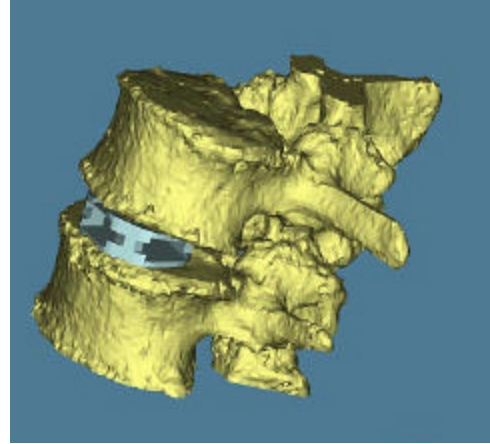


Figure 5: Anatomic fitting of the inter-vertebral implant

The effective Young's module (E_{TiHA}), the Poisson ratio (ν_{TiHA}), and the strength (σ_{TiHA}) of TiHA composite were derived from the composite micro-mechanical model [15], and expressed in Equation (1) to Equation (3), respectively. In which, Equation (1) represents the formula of effective Young's module of composite consisting of titanium particle embedded in the hydroxyapatite matrix. Equation (2) and Equation (3) represent the mathematical formulation of Poisson ratio and strength derived based on the composite's Rule of Mixture.

$$E_{TiHA} = E_{HA} \left\{ \frac{E_{HA} + (E_{Ti} - E_{HA})V_{Ti}^{2/3}}{E_{HA} + (E_{Ti} - E_{HA})V_{Ti}^{2/3}(1 - V_{Ti}^{1/3})} \right\} \quad (1)$$

$$\mathbf{u}_{TiHA} = \mathbf{u}_{Ti}V_{Ti} + \mathbf{u}_{HA}V_{HA} \quad (2)$$

$$\mathbf{s}_{TiHA} = \mathbf{s}_{Ti}V_{Ti} + \mathbf{s}_{HA}V_{HA} \quad (3)$$

in which, E_{Ti} and E_{HA} denote the Young's modules, ν_{Ti} and ν_{HA} denote the Poisson ratios, and V_{Ti} and V_{HA} denote the volume fractions of TiHA composite for titanium and hydroxyapatite, respectively. The material properties of hydroxyapatite and titanium and the results of the calculation are listed in Table 1. The volume fractions of both constituents V_{Ti} and V_{HA} in TiHA were all assumed to be 0.5 in the calculation.

It should be pointed out that the model predicted data can only be served as reference data since the actual properties of the TiHA composite are process-dependent and related to the process parameters such as the synthesized temperature, pressure, and the micro-structure of the constituents (shape and size). The realistic TiHA properties should be obtained through experimental tests.

Table 1 - The elastic properties of TiHA composite

Material	E in GPa (Msi)	Poisson ration ν	Strength in compression (MPa)
Hydroxyapatite [14]	34.0 (5.0)	0.28	75
Titanium [12]	117.0 (17.0)	0.33	600
TiHA	65.5 (9.6)	0.305	337.5

In the finite element analysis, Pro/M software first converted the Pro/E implant CAD model into a FEA model. The AUTOMECH module in Pro/M was used to automatically generate a total of 728 tetrahedral elements. The meshing and the elements are shown in Figure 6. The boundary conditions, constraints, and loading were then applied to the FEA model. To simulate the deformation of the implant within the vertebrae, we allowed the top and bottom surfaces of the implant to be free to deform and only completely constrained three individual nodes at the bottom surface to ensure the model stability in the finite element analyses. The pressure loading were applied on the top and bottom surfaces to mimic the pressure imposed by the vertebrae. The constraints and loading conditions for the analysis are schematically shown in Figure 7.

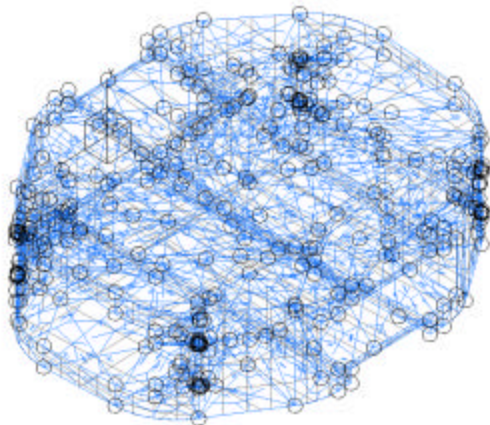


Figure 6: FEA mesh of the implant

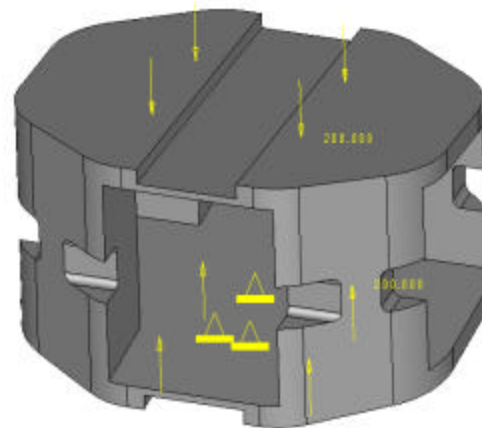


Figure 7: Constraints and loading

Extra care must be exercised in determining the loading imposed on the implant. Anatomically, the vertebrae consist of a thin shell of hard cortical bone surrounding a network of softer trabecular bone. Under normal physiological conditions, most of the load on the vertebral body is slightly anterior to its midpoint. Thus, the cortical bone in this area tends to be denser and stronger [16]. Physiological loads on lumbar vertebrae are difficult to measure. From a design point of view, this does not provide sufficient information to determine the loading applied to the implant from the weight of the body or from a weight that is lifted. The center of gravity in the human body is anterior to the spine, so the resultant moments must be balanced out by muscles such as the spinal erectors. This may result in a higher load exerted on the spine. In a recent landmark experiment, load cells were implanted into the lumbar spine of baboons. In some cases, loads were so high that they were beyond the measuring capacity of the load sensor. For example, standing upright resulted in a load of 690 N for an animal weighing 390 N [17].

In our analysis, we assume that the total pressure load passing through the lumbar vertebrae is applied on both top and bottom surfaces of the implant model as shown in Figure 8. Since we do not know exactly how the pressure is distributed on the surfaces, we studied two possible pressure patterns, as shown in Figure 8. One pattern assumes that the pressure is uniformly distributed on the surfaces. As shown in Figure 8a, $p_{\text{uniform}} = 4.33$ MPa, which is equivalent to 2000 N total pressure load. The other assumes that the magnitude of the applied pressure varies linearly with the inclined angle of the surfaces, for example, $p_{\text{max}} = 7.447$ MPa, and $p_{\text{min}} = 1.242$ MPa, which is also equivalent to 2000 N total pressure load, as shown in Figure 8b. The mechanical properties of in vivo vertebrae may vary due to the bone mineral density and the variations in morphology. The maximum pressure applied on the surface, $p_{\text{max}} = 7.447$ MPa, is between the strength of cortical bone (compression strength = 195 MPa) and the strength of cancellous bone (compression strength = 2.8 MPa). Therefore, if the cortical bone is in good condition, we expect it will be able to withstand the applied pressure, i.e., to support the inter-vertebral implant without collapsing the bone.

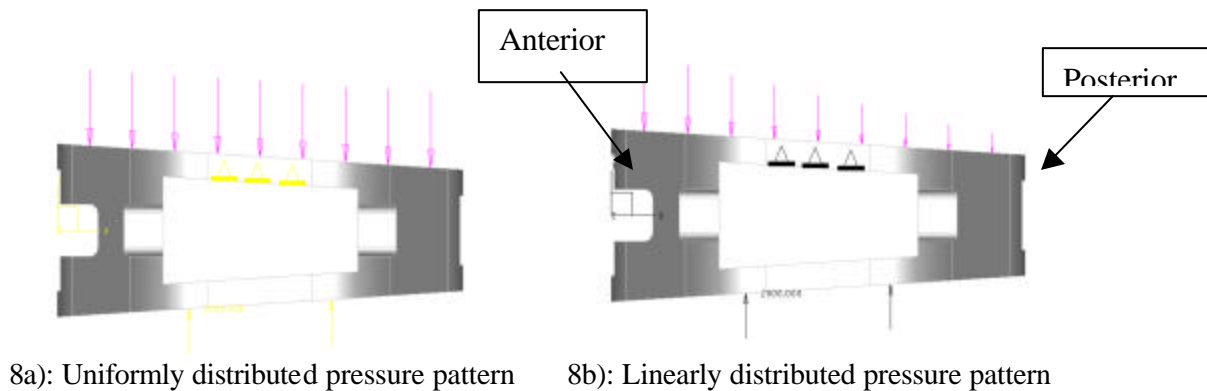
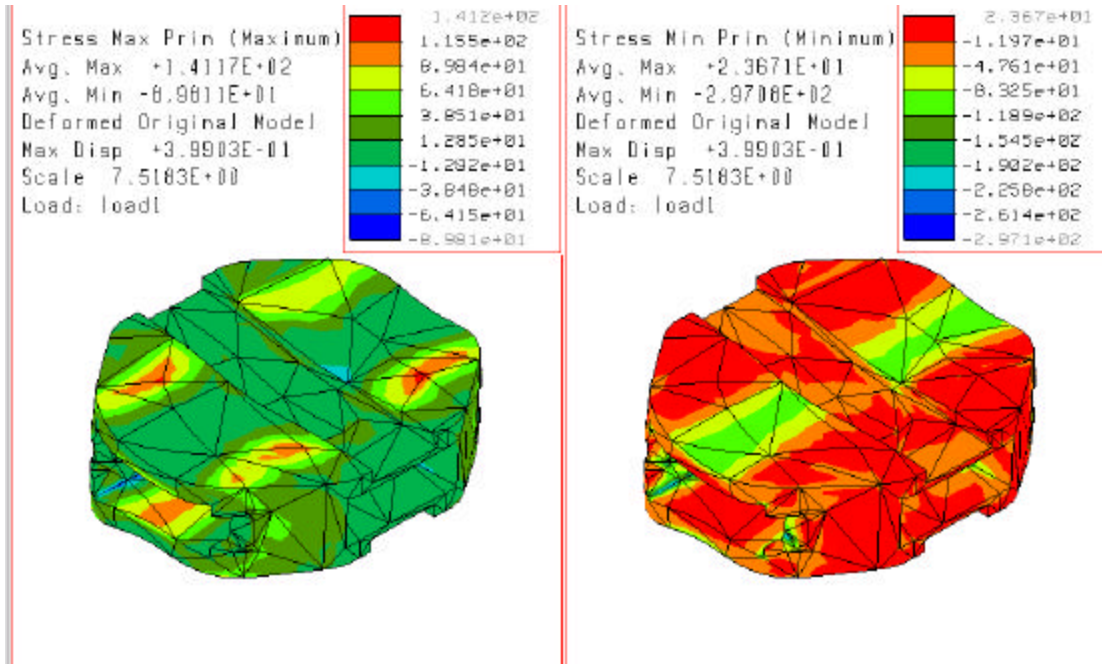


Figure 8: - Pressure patterns

In the finite element analyses presented in this study, we assume the mechanical properties of the TiHA to be linearly elastic with the properties listed in Table 1. Using Pro/M, the P-version high order interpolating polynomials was adopted for the solution convergence. In our case studies, 6 p-loop passes were performed before all elements satisfied the convergence condition. The results of the finite element analysis are represented in Figure 9 and Figure 10, respectively. Figure 9 displays a contour representation of the maximum principal stress and minimum principal stress distributed in the inter-vertebral implant subject to a uniformly distributed pressure loading. Figure 10 shows the similar contour representation, but for a linearly distributed pressure-loading condition.

A summary of the maximum and minimum principal stresses calculated from the finite element analyses for the inter-vertebral implant are listed in Table 2. These values are used to verify if the implant satisfies the strength requirement. It can be shown that all calculated maximum stresses in the implant are below the strength of the TiHA composite, for example, σ_{max} (minimum principal) = 297.1 MPa < 337.5 MPa (TiHA strength). With this, we assume that the designed inter-vertebral implant with the TiHA composite at a 50/50 composition will probably be structurally strong enough to withstand the specified loading. However, as discussed

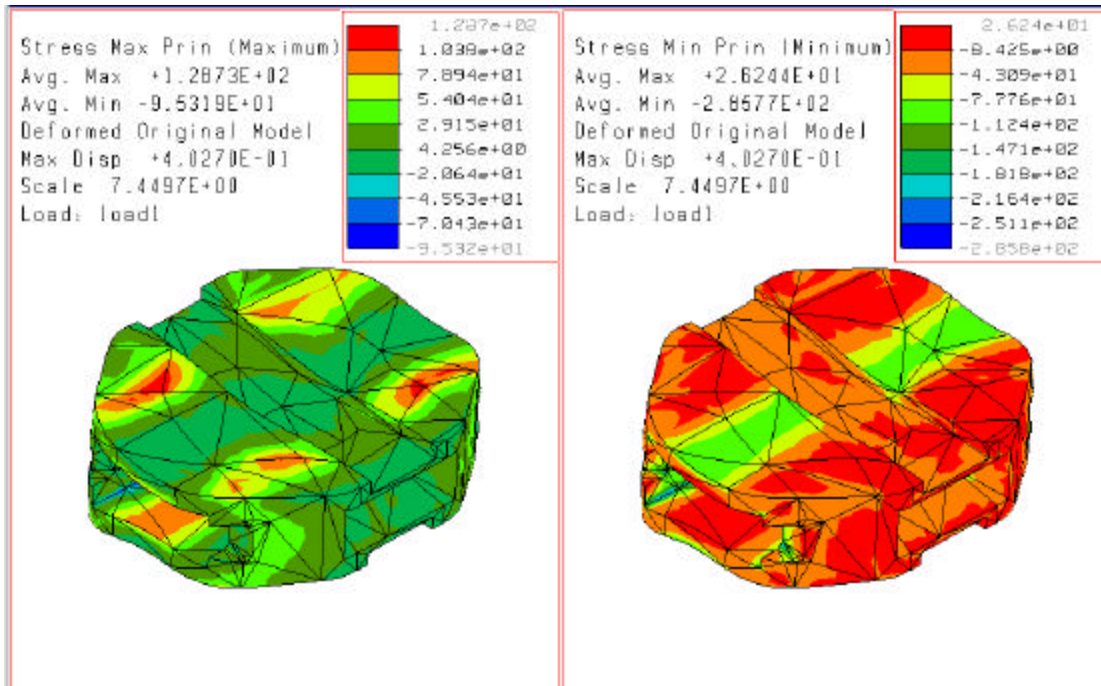
before, the property of the implant is influenced by many processing factors and the important property data should be examined through appropriate experimental testing.



Maximum principal stress

Minimum principal stress

Figure 9: Contour representation of the maximum and minimum principal stresses under uniformly distributed pressure loading



Maximum principal stress

Minimum principal stress

Figure 10: Contour representation of the maximum and minimum principal stresses under linearly distributed pressure loading

Table 2 – Finite element results in the implant

Load pattern	Total load	σ_{\max} (Max. principal)	σ_{\min} (Min. principal)
Uniform pressure	2000 N	141.2 MPa	-297.1 MPa
Linear pressure	2000 N	128.7 MPa	-285.8 MPa

4. 3D Printing of Vertebrae and Inter-Vertebral Implants

Titanium and hydroxyapatite can be made into a composite by the powder consolidation method. A volume fraction of 50/50 (titanium and hydroxyapatite powders) is mixed using a ball milling operation. After undergoing an appropriate thermal treatment, the synthesized TiHA composite will provide the hydroxyapatite with more ductility while still providing the osteo-conductive feature of pure hydroxyapatite. In addition to its biological effects, the TiHA composite material will have a higher toughness (less brittle) than pure hydroxyapatite as well as a good fatigue property. This is particularly beneficial for spinal fusion since most spinal implants are damaged due to the fatigue failure.

The rapid prototyping of TiHA implants involves primarily two major processes: 1) 3D Printing of the green part; and 2) Hot Iso-static Pressing (HIP) of the TiHA component. The flow chart of the processes is schematically presented in Figure 11. The work completed in the first process, i.e., 3D printing of vertebrae and inter-vertebral implants, is reported in this study. A general sintering procedure of the HIP post-process will be briefly described. However, research work in the second process, particularly on the binding mechanism of the TiHA particles and the effect of the post-HIP process on the biological and mechanical behavior of the TiHA component are still under investigation and the results will be reported in the future.

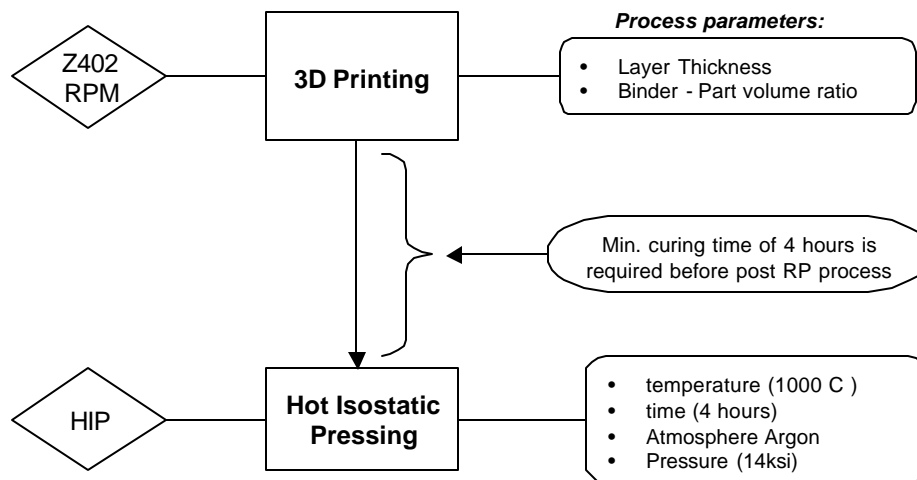


Figure 11: Flow chart of rapid prototyping of TiHA implant

In the beginning of the 3DP process, the *stl* files generated from MIMICS for vertebrae anatomy and from Pro/E for the inter-vertebral implant were converted into a Z402 system Build File (*.bld) and the data was temporarily stored in the form of slices. The slice data were

interpreted and put together by a 3D printing system to produce the prototypes. The Z402 system consists of 2 powder bays, a feed bay, a build bay, and a binder spray head with a cartridge. The slice data, obtained from the Build File, are input into the machine. The binder spray head initially sprays the binder on to the first powder layer (depending on the cross-section of the part at that particular section). As the binder head moves across the 2 bays, it rolls a layer of powder (depending on the specified layer thickness) from the feed bay to the build bay. This process continues, layer by layer, until the entire prototype is built. The printed prototype, or green part, is then removed from the build bay and cleaned using compressed air to remove the excess powder. Furthermore, the green part is subjected to a post-process by infiltrating wax or polymer resin to give additional strength before sending to HIP process to sinter final TiHA component.

The vertebrae were prototyped using zp-11 powder as the build material and zp-07 as the binder. The inter-vertebral implant was prototyped using hydroxyapatite powder as the build material. Both the vertebrae and the implant prototypes were post-processed by infiltrating the model with molten wax and polymer resin to provide additional strength after the printing. The specifications and the process parameters of the 3D Printing are listed in Table 3.

Table 3 - 3D Printing specifications and process parameters

Base material (powder)	Hydroxyapatite / zp-11
Binder	zb-07
Layer thickness (range)	0.01” to 0.0035”
Binder volume (percentage of total volume)	Shell / Core Vertebrae: 14% / 7% Implant: 14% / 14%
Build Speed	1” / hour along z-axis
Accuracy	0.5% along X-Y axes, 1% along Z-axis

The compacted green part is further subjected to sintering by HIP process. The HIP process applies heat and pressure within an enclosed vessel to consolidate or condense materials such as castings. Heat is introduced via molybdenum resistance elements and pressure is supplied by high pressure pumps forcing argon, an inert gas, into the vessel. As the heat softens the castings, the gas pressure exerts a force equally on all surfaces, causing the porous casting to compress to full density. Crucibles HIP vessel and Molybdenum resistance furnaces are used to provide HIP temperatures ranging from 900°F to 2250°F (1230°C) for different metallic alloys, at a gas pressure up to 15,000 psi (103 MPa). In the attempt to sinter TiHA component, the vacuum glass tubes are heated to a temperature of 1000 °C with a pressure of 14ksi for a period of 4 hours in an argon atmosphere. The applied temperature profile of the HIP process is shown in Figure 12.

5. Summary and Conclusion

A case study using the rapid prototyping technology to assist in the design and development of inter-vertebral implants for spine fusion procedures was demonstrated. The process of the design and the implant development, the biological and mechanical constraints, the development of the 3D reconstructive anatomy model and the inter-vertebral implant CAD model, and the application of the models with integrated finite element analysis for implant structural analysis were presented. 3D Printing of the anatomy model and the implant model,

along with the prototyping and post sintering process were described. The application of the prototyping model in assisting in the inter-vertebral anatomic fitting, in guiding the implant's geometric design, and in helping with the virtual surgical planning was demonstrated. Based on the designed implant and anatomic models, finite element analyses were conducted to understand the implant's mechanical properties and structural stability, and the results were also presented.

We were able to generate vertebral anatomy from CT scanned images of a human spine through MIMICS. MIMICS was also used to edit the 3D images and to measure the anatomic geometry of the vertebrae in order to determine the key dimensional parameters for implant design. An *stl* file was created from the edited image to make a prototype of the spine segment. Surface details of the lumbar vertebrae were accurately modeled, but it was not possible to model any of the interior details (such as the trabecular bone) due to the inherent precision of the CT scanner.

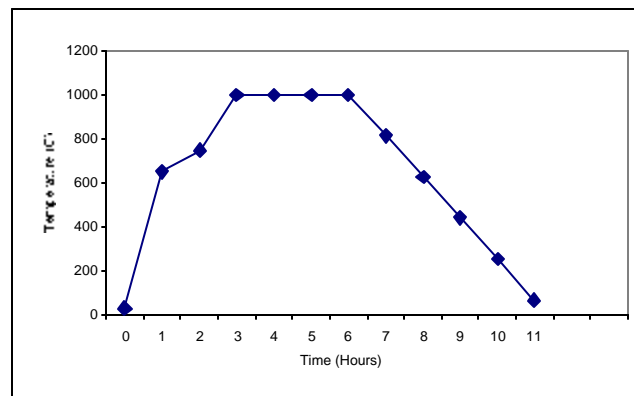


Figure 12: Temperature profile in HIP process

In order to verify the anatomic fitting of the designed inter-vertebral implant, we converted the Pro/E implant model into an *stl* format and input it into MIMICS, as shown in the 3D rendered image in Figure 5. The computer simulation of the positioning and the placement of the designed implant with the patient's vertebrae can be used as an effective tool to help surgeons to make the pre-operative plan and to practice the implantation.

The structural analyses were performed to the TiHA implant structure by using Pro/M software. It was found that the maximum stress (297 MPa) occurred within the implant under the applied loading (2000 N). This value was below the strength (375 MPa) of the TiHA implant. We need to pointed out that for results presented in the analysis and comparison, we used the mechanical properties of the composite obtained from the model prediction, not from the experimental testing. In addition, we were not able to analyze the vertebral anatomy because the CT scanned images were not be able to provide the interior detail of the trabecular structure inside the vertebral body. Without these detail, we can not generate the needed CAD and FEA models.

6. Acknowledgement

We gratefully acknowledge the support from NSF 9980298 project during the course of this study.

References

1. Langer, R. and Vacanti, J. Tissue Engineering. *Science* 260: (1993) 920-925
2. Boden, S.D. Biology of Lumbar Spine Fusion and Use of Bone Graft Substitutes: Present, Future, and Next Generation. *Tissue Engineering* 6(4): (2000) 383-399.
3. Haher, T.R. et al. An *In Vitro* Biomechanical Investigation of Spinal Interbody Fusion Devices. Proceedings of the 14th Annual Meeting of NASS. Chicago: (1999) p. 70-72.
4. Alexander, H. et. al. Classes of Materials used in Medicine. Biomaterials Science. Ed. Ratner et. al. Academic Press; San Diego (1996) P. 74.
5. Bauer, T.W., Geesink, R.C., Zimmerman, R. and McMahon, J.T., "Hydroxyapatite-coated femoral stems, Histological analysis of components retrieved at autopsy," *J. Bone Joint Surg.*, 73: (1991) 1439-52.
6. Cook, S.D., Thomas, K.A., Kay, J.F. and Jarcho, M., "Hydroxyapatite-coated titanium for orthopedic implant applications," *Clin Orthop*, (1988) 232, 225-43.
7. Klein, C.P.A.T., Patka, P., Wolke, J.G.C., de Blicke-Hogervorst J.M.A., and de Groot K., "Long-term in vivo study of plasma-spray coatings on titanium alloys of tetracalcium phosphate, hydroxyapatite and alpha-tricalcium phosphate," *Biomaterials*, (1994) 15, 146-50.
8. Yamada, K., Imamura K., Itoh, H., Iwata, H., and Maruno, S., "Bone bonding behavior of the hydroxyapatite containing glass-titanium composite prepared by Cullet method," *Biomaterials*, 22, (2001) 2207-2214.
9. Bloebaum, R.D. and Dupont, J.A., "Osteolysis from a press-fit hydroxyapatite-coated implant: a case study," *J. Arthroplasty*, 8, (1993) 195-202.
10. Paschalis, E.P., Zhao, Q., Tucker, B.E., Mukhopadhyay, S., Bearcroft, J.A., Beals, N.B. et al., "Degradation potential of plasma-sprayed hydroxyapatite-coated titanium implants," *J. Biomed Mater Res*, 29, (1995) 1499-505.
11. Shen, W.J., Chung, K.C., Wang, G.J., and Mclaughlin, R.E., "Mechanical failure of hydroxyapatite-and polysulfone-coated titanium rods in a weight-bearing canine model," *J. Arthroplasty*, 7, (1992) 43-49.
12. Moroi, H.H., Okimoto, K., Moroi, R., and Terada, Y., "Numeric approach to the biomechanical analysis of thermal effects in coated implants," *Int. J. Prosthodont*. 6: (1993) 564-572.
13. Sun, W., Lal, P., "Recent Development on Computer-Aide Tissue Engineering," *J. of Computer Methods and Programs in Biomedicine*, *in press*.
14. Grenoble, D.E., Katz, J.L., Dunn, K.L., Gilmore, R.S., and Murty, K.L., "The elastic properties of hard tissues and apatites," *J. Biomed. Mater., Res.*, 6(3): (1972) 221-223.
15. Jones, R., "Mechanics of Composite Materials," Taylor & Francis, Philadelphia, PA, 1999
16. White, A., and Panjabi, M. *Clinical Biomechanics of the Spine*. Lippincott Williams & Wilkins. Philadelphia (1990) P. 43.
17. Ledet, E. et al. Real-Time *In Vivo* Loading in the Baboon Lumbar Spine Using an Interbody Implant Load Cell. Proceedings of the 14th Annual Meeting of NASS. Chicago: (1999) 202-204.